Journal of Photochemistry and Photobiology A: Chemistry 208 (2009) 186–194

Contents lists available at ScienceDirect

Journal of Photochemistry and Photobiology A: Chemistry

journal homepage: www.elsevier.com/locate/jphotochem

Kinetics and mechanism of the tropospheric reaction of tetrahydropyran with Cl atoms

B. Ballesteros, A.A. Ceacero-Vega, A. Garzón, E. Jiménez, J. Albaladejo*

Universidad de Castilla – La Mancha, Departamento de Química Física, Facultad de Ciencias Químicas, Avenida Camilo José Cela, s/n, 13071 Ciudad Real, Spain

ARTICLE INFO

Article history:
Received 22 July 2009
Received in revised form 8 September 2009
Accepted 14 September 2009
Available online 19 September 2009

Keywords:
Cl atoms
Tetrahydropyran
Kinetics
Atmospheric reaction
Ab initio calculations
Mechanism

ABSTRACT

Relative rate coefficients for the gas-phase reaction of chlorine atoms (Cl) with tetrahydropyran (THP) have been determined by Fourier transform infrared (FTIR) spectroscopy and gas chromatography coupled to a mass spectrometer (GC–MS). The averaged rate coefficient is $(2.21 \pm 0.32) \times 10^{-10}$ cm^3 molecule^{-1} s^{-1} (with 2σ uncertainty) and was obtained using different reference compounds, Cl precursors, and bath gases at 740 ± 5 Torr and 298 ± 2 K. Products of the title reaction were identified and quantified by solid-phase microextraction (SPME) coupled to a GC–MS. Additionally, the first step of the reaction was theoretically studied by *ab initio* calculations. Reaction mechanism seems to proceed mainly by the H-abstraction from α and γ positions. THP tropospheric lifetime is estimated from the rate coefficient reported here. The atmospheric implications of the Cl reactivity are also discussed.

1. Introduction

Ethers, which are used as industrial solvents and additives to unleaded gasoline to increase the octane rating, are emitted to the atmosphere contributing to the formation of photochemical smog [1]. Given the widespread use of oxygenated compounds as solvents and additives, it is important to characterize the sink of these compounds. Tetrahydropyran (THP, $(CH_2)_5O$) is a cyclic ether used in the synthesis of organic and natural products as reactive and solvent [2–5]. Also THP is part of the chemical composition of antimicrobial compounds [6] and metabolites [7]. To understand and evaluate the environmental impact of ethers, a detailed study of the kinetics, products and mechanisms of their atmospheric degradation is required.

Ethers are generally more reactive in the atmosphere than alkanes of similar chain length [8]. The primary atmospheric fate of organic compounds, in general, is the reaction with hydroxyl radicals (OH) in the gas phase. Only two kinetic studies on the OH-initiated reaction of THP have been reported in the literature. Dagaut et al. [9] have reported a rate coefficient of $(1.38 \pm 0.07) \times 10^{-11}$ cm^3 molecule^{-1} s^{-1} measured by Flash Photolysis/Resonance Fluorescence (FP/RF) and Moriarty et al. [10] have reported a rate coefficient of $(1.15 \pm 0.06) \times 10^{-11}$ cm^3 molecule^{-1} s^{-1} by a relative technique and $(1.23 \pm 0.04) \times 10^{-11}$ cm^3 molecule^{-1} s^{-1} by pulsed laser photolysis/laser induced fluorescence (PLP/LIF). To our knowledge there is no previous information in the literature about the reaction of this cyclic ether with chlorine atoms (Cl). In recent years, the oxidation by Cl atoms has gained great importance in the study of atmospheric reactions because they may exert some influence in the boundary layer, particularly in marine and coastal environments, and in the Arctic troposphere during springtime [11–14]. Atomic chlorine, generated by the photolysis of molecular chlorine released to the atmosphere via reactions in sea salt particles, can then contribute to the oxidation of organic compounds in the marine boundary layer [15]. The rate coefficients obtained for the degradation of organic compounds with Cl atoms are often a factor of 10 higher than the corresponding OH rate coefficients. In the marine boundary layer, concentrations of Cl_2 of up to 150 parts per trillion by volume (150 pptv) [16] and photolyzable chlorine of up to 250 pptv [17] have been reported. In the Arctic, high concentrations of photolyzable chlorine (up to 100 pptv) have been measured [18]. Photolysis of these species is expected to result in peak Cl atom concentrations as high as 10^5 atoms cm^{-3} or more in the marine boundary layer [16]. High levels of chlorine were also detected in polluted urban areas close to structural ceramic industries [19].

In this paper, a set of physicochemical techniques was used to study the kinetics and mechanism of the tropospheric reaction of THP with Cl atoms. The relative rate coefficient for the Cl-initiated oxidation of THP at 298 ± 2 K is reported for the first time. Major primary oxidation products have been identified and quantified and *ab initio* calculations have been performed in order to identify

* Corresponding author. Tel.: +34 926 29 53 27; fax: +34 926 29 53 18.
E-mail address: Jose.Albaladejo@uclm.es (J. Albaladejo).

1010-6030/$ – see front matter © 2009 Elsevier B.V. All rights reserved.
doi:10.1016/j.jphotochem.2009.09.014

the main reaction pathway. Finally, the mechanistic implications and tropospheric fate of this cyclic ether are also discussed. The kinetic data obtained in this study will extend the database of available information for the reactions of ethers that are released to the troposphere.

2. Experimental

2.1. Relative kinetic method

The relative Cl-kinetic measurements and the detection of reaction products were performed in two environmental chambers equipped with FTIR and GC–MS. A detailed description of the experimental set-up with FTIR detection and the kinetic analysis performed has previously been presented for the reaction of linear and branched alcohols with Cl atoms [20]. Thus, the experimental system will be only briefly described here. It consists of a multipass 16 L borosilicate glass cylinder reaction chamber, homogeneously surrounded by 4 UV fluorescent lamps (Philips TL-K 40 W, λ_{max} = 365 nm), coupled to a Nexus Thermo Nicolet FTIR spectrometer equipped with a liquid nitrogen cooled mercury cadmium telluride (MCT) detector for on-line infrared spectroscopy. The total path length is 96 m. The spectra were obtained by coadding 64 scans recorded at 2 cm^{-1} instrumental resolution in the 650–4000 cm^{-1} range. Reactants were introduced directly into the cell by expansion from a glass manifold system and mixed in synthetic air or helium at 298 ± 2 K and 740 ± 5 Torr of total pressure.

The experimental system with GC–MS detection has recently been set-up. The environmental chamber consists in a 100 L or 200 L Teflon bags, surrounded by 8 UV lamps (Philips TL-K 40 W). Gas samples were analyzed by GC (Thermo Electron Co., model Trace GC Ultra) coupled to a mass spectrometer (Thermo Electron Co., model DSQ II). The gas sample was directly introduced into the GC with an automatic 6 ways valve and a 1 mL loop evacuated with a vacuum pump.

Chlorine atoms were produced by the broad-band UV photolysis of Cl_2 or $SOCl_2$ in the bath gas (synthetic air or He). UV radiation was produced by the lamps homogeneously arranged around the outside of the glass cell and the Teflon bag. Total irradiation times were shorter than 180 min for Cl_2 and shorter than 3 min for $SOCl_2$; these times guarantee a reagent conversion of 80–90%. The irradiation time is not continuous for the GC–MS system and the analysis is performed when the lamps are off. Experiments were also performed in the absence of radiation to check for dark reactions and wall losses. During 'blank test experiments' the losses of reactants were much lower than 1% during the time of a typical experiment and therefore the influence of the reaction rate coefficients were considered to be negligible for the results presented here. The photolysis of THP and reference compounds was previously tested and no significant loss was detected.

Gas-phase concentrations, both in the FTIR cell and in the Teflon bag, were calculated considering the partial pressure of the gas in a cylinder of calibrated volume and the total volume of the reactor. Concentrations in the reaction chamber for THP and the reference compound (propene, 1,3-butadiene, 1-butene, and ethene) ranged from 9 to 18 ppm, while for the precursors of Cl atoms (Cl_2 and $SOCl_2$) ranged from 8 to 16 ppm. Reactants were left to homogenize in the reactor for ~30 min prior to irradiation. After each experiment, the reaction chamber was cleaned out by repeated purge-pump cycles until the reactants and/or products were not detected.

The rate coefficient used for Cl + propene reaction was the recommended value by the IUPAC [21], 2.3×10^{-10} cm^3 $molecule^{-1}$ s^{-1} (we have added a 10% of error for estimating σ). For the rate coefficient of Cl atoms with 1,3-butadiene the reported value by Ragains and Finlayson-Pitts [22] at 760 Torr of air and 298 K $(4.20 \pm 0.40) \times 10^{-10}$ cm^3 $molecule^{-1}$ s^{-1} was used. The Cl rate coefficient used for 1-butene was $(3.00 \pm 0.40) \times 10^{-10}$ $molecule^{-1}$ s^{-1} obtained recently by Orlando et al. [23] at 298 K near 1 atm. For ethene the recommended value by the IUPAC [21], 1.1×10^{-10} cm^3 $molecule^{-1}$ s^{-1} (we have added a 10% of error for estimating σ), was used.

2.2. Product study

The products formed in the reaction of Cl atoms with THP under atmospheric conditions (298 ± 2 K and 740 ± 5 Torr of synthetic air) were investigated using a 200 L Teflon bag and employing the technique of solid-phase microextraction (SPME) coupled to a GC–MS.

SPME is a simple and effective adsorption and desorption technique, which eliminates the need of using solvents or complicated apparatus for concentrating volatile or non-volatile compounds in liquid samples or headspaces [24,25]. It is compatible with analyte separation and detection by GC and high-performance liquid chromatography (HPLC), and provides a linear response for a wide range of analyte concentrations [25]. This technique was introduced to analyse relatively volatile compounds in the environmental field, but recently its use has been extended to the analysis of a great variety of matrices: gas, liquid, and solid, and to a wide range of analytes from volatile to non-volatile compounds [25]. Recently, SPME has been used in the study of atmospheric reactions of several organic compounds [26–30].

In this work, a 50/30 μm divinylbenzene/carboxen/polydimethylsiloxane fibre was used. The coated fibre was inserted into the Teflon chamber and exposed during typically 20 min to the chamber contents. Then, SPME fibre samples were thermally desorbed in the heated (270 °C) GC injection port and the products were analysed by mass spectrometry. The identification of the products was made by analysis of the mass spectrum and by comparison with a library of spectra. When possible, the identification was made by comparing with the retention time of a pure sample of the detected product; when this identification was not possible a tentative assignment was proposed. Under the conditions used here the SPME/GC–MS response was linear with the analyte concentration. No carryover was observed for any of the compounds upon a second injection, indicating a complete recovery of the fibre. The fibre was used immediately after desorption for the next sampling.

2.3. Chemicals

The liquid chemicals employed in these experiments were supplied by Aldrich with the purities given in brackets: tetrahydropyran (99%), δ-valerolactone (99%), γ-butyrolactone (99%), tetrahydro-4H-pyran-4-one (99%), tetrahydro-4-pyranol (98%), $SOCl_2$ (99%), and 1-butene (99%). All liquid reagents were degassed by repeated freeze–pump–thaw cycles prior use. Gaseous reagents were used as supplied: Cl_2 (99.8%, Praxair), 1,3-butadiene (99%, Aldrich), propene (99%, Aldrich), and ethene (99.9%, Fluka).

3. *Ab initio* calculations

The reaction of Cl atoms with THP can proceed by H-abstraction from three different positions with respect to the O atom. In order to evaluate the relative importance of these possible reaction pathways, *ab initio* calculations on the first step of the reaction were carried out using the Gaussian 03 [31] set of programmes running on the resources of the Supercomputing Service of the University of Castilla-La Mancha.

Firstly, geometries of reactants and transition states (TS) were optimized at Möller Plesset second-order perturbation theory (MP2) with 6 31G* basis sets. The nature of the stationary points was assessed through the frequencies of the normal vibrations cal-

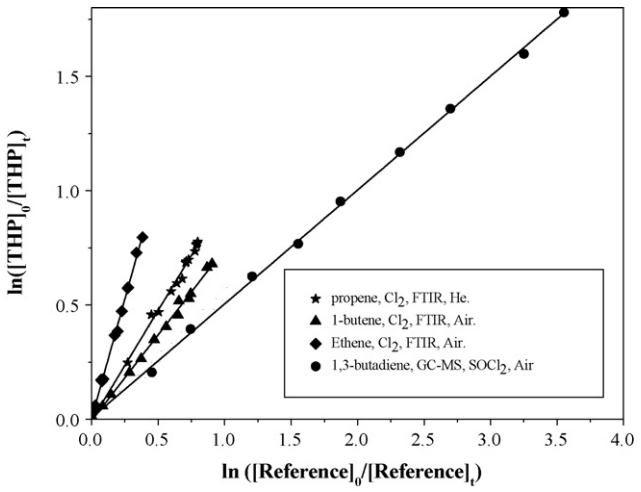

Fig. 1. Examples of relative rate data for the reaction of THP with Cl atoms using different reference compounds, Cl precursors, detection technique, and bath gas at 298 ± 2 K and 740 ± 5 Torr of total pressure.

culated with the energy analytical second derivatives. First order saddle points, which are related to transition states, show an imaginary value for the frequency associated to the eigenvector describing mainly the product formation step. Real minima of the potential energy hypersurface, which are related to stable species, show all positive real values for vibrational frequencies.

For open-shell structures, spin contamination may affect the energy and geometry of the system [32,33] and increases, in general, as a bond stretches, which turns out to be interesting for transition states that contain elongated bonds. This effect must be taken into account if total spin $\langle S^2 \rangle$ differs from $s(s+1)$ by more than 10%, s being 1/2 times the number of unpaired electrons. In our system, the expected spin values $\langle S^2 \rangle$ before annihilation of contamination differ from the theoretical ones, 0.75, by no more than 5%. Therefore, spin contamination can be considered negligible. The energies of reactants and transition states have been computed at quadratic configuration interaction, i.e., QCISD(T) method on MP2/6-31G* geometries. Both geometries and energies were calculated using frozen core approximations.

VeryTight and CalcFC criteria [31] were taken for surpassing the convergence difficulties in the calculation in the case of transition states. For each reactant and transition state, zero-point energy and different thermal corrections of the QCISD(T) energy values were considered in order to calculate the thermodynamical functions at 298.15 K. Activation energies (E_a) at 298.15 K were calculated from activation enthalpies ($\Delta H^{\#}$) using the expression $E_a = \Delta H^{\#} + 2RT$. The same strategy of calculation has been used in our laboratory in previous studies on the reactions of Cl atoms with linear alcohols [33] and thiols [34]. The usual accuracy of this type of calculations is about 1–1.5 kcal/mol [35,36].

4. Results and discussion

4.1. Relative rate coefficient measurements

The relative disappearance rates of THP and the reference organic compound were measured in the presence of Cl atoms:

$$\mathrm{Cl} + \mathrm{THP} \rightarrow \text{products} \qquad k_1 \tag{1}$$

$$\mathrm{Cl} + \mathrm{REF} \rightarrow \text{products} \qquad k_{\mathrm{ref}} \tag{2}$$

where REF is a reference compound for which the rate coefficient k_{ref} is reliably known. Provided that THP and the reference compounds react only with Cl, the following expression can be derived:

$$\ln\frac{[THP]_0}{[THP]_t} = \frac{k_1}{k_{\mathrm{ref}}}\ln\frac{[\mathrm{REF}]_0}{[\mathrm{REF}]_t} \tag{3}$$

where the subscripts 0 and t indicate the concentration at the beginning of the reaction and at a reaction time t, respectively. k_1/k_{ref} is the slope of the straight line obtained by the linear least-squares analysis of the two sets of decay data. Some experiments were performed in the absence of Cl precursor and/or UV light in order to determine the possible contribution to the rate coefficients due to the wall losses of the ether and the reference compounds and photolysis. Under the conditions used in this work wall losses of the compounds were not observed. Some plots of Eq. (3) are given in Fig. 1, showing in all cases a good linearity.

Table 1 shows the ratios k_1/k_{ref} where the error limits given include the precision of the fit to our experimental data (twice the standard deviation, $\pm 2\sigma$). The errors given for k_1 are a combination of the 2σ statistical errors from the linear regression analyses and the statistical error propagation, taking into account the error of reference compound rate coefficient or a σ of 10% if the error has not found in the bibliography. The experiments were performed using air and helium as bath gases, and no influence on the rate coefficient was observed. In addition, no influence of the Cl precursor used (Cl_2 or $SOCl_2$) on the relative rate coefficient was observed, as it is shown in Table 1. The average value of k_1 obtained from all data sets was $(2.21 \pm 0.32) \times 10^{-10}$ cm^3 molecule^{-1} s^{-1}.

4.2. Theoretical features

The THP molecule belongs to C_{2v} point group of symmetry, and thus only three possible attacks in the hydrocarbon ring (α, β, and γ positions) have been considered.

Table 1
Rate coefficient ratios and the obtained relative rate coefficients for the reaction of Cl atoms with THP at 298 ± 2 K and 740 ± 5 Torr of air.

Reference compound	Bath gas	Detection technique	Cl precursor	$(k_1/k_{\mathrm{ref}}) \pm 2\sigma$	Runs	$(k_1 \pm 2\sigma) \times 10^{10}$ (cm^3 molecule^{-1} s^{-1})
Propene[a]	Air	FTIR	Cl_2	0.94 ± 0.01	6	2.17 ± 0.28
	Helium			0.95 ± 0.01	5	2.19 ± 0.29
1,3-Butadiene[b]		FTIR	Cl_2	0.56 ± 0.01	5	2.35 ± 0.23
	Air	GC–MS		0.51 ± 0.01	4	2.14 ± 0.21
		GC–MS	$SOCl_2$	0.52 ± 0.01	4	2.18 ± 0.21
1-Butene[c]	Air	FTIR	Cl_2	0.74 ± 0.02	2	2.22 ± 0.30
Ethene[d]	Air	FTIR	Cl_2	2.08 ± 0.05	2	2.29 ± 0.46
					Average	2.21 ± 0.32

[a] k(propene) = $(2.3 \pm 0.46) \times 10^{-10}$ cm^3 molecule^{-1} s^{-1} [21] (see text).
[b] k(1,3-butadiene) = $(4.20 \pm 0.40) \times 10^{-10}$ cm^3 molecule^{-1} s^{-1} [22].
[c] k(1-butene) = $(3.00 \pm 0.40) \times 10^{-10}$ cm^3 molecule^{-1} s^{-1} [23].
[d] k(ethene) = $(1.1 \pm 0.22) \times 10^{10}$ cm^3 molecule^{-1} s^{-1} [21] (see text).

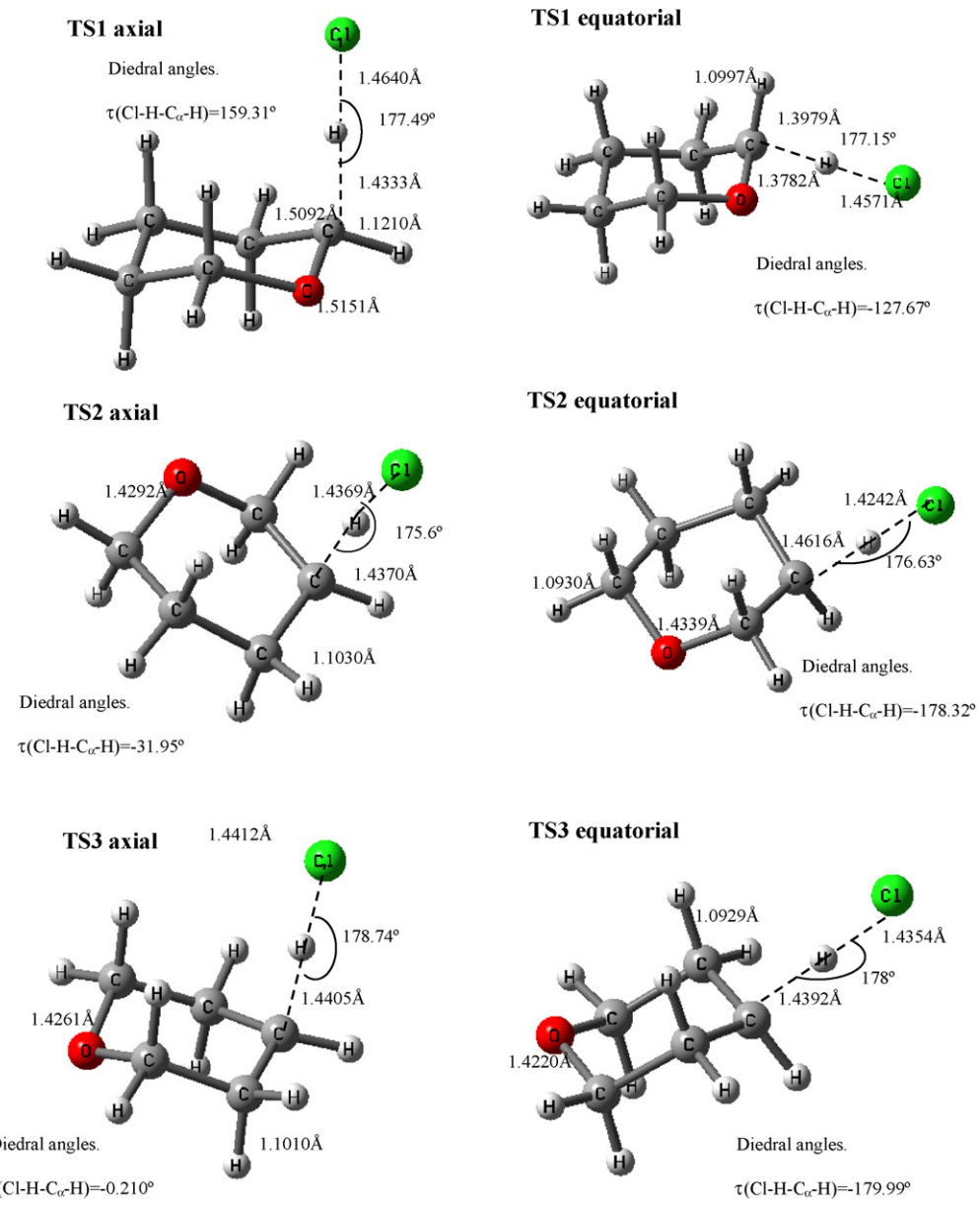

Fig. 2. The most important structural parameters of the transition states calculated by the *ab initio* method described in the text.

In the Cl attacks to the hydrogen atoms in α position, two transition states are possible (TS1): one equatorial ($TS1_{eq}$) and one axial ($TS1_{ax}$), which are characterized by an imaginary frequency of 1049*i* and 540*i* cm^{-1}, respectively. These normal modes are pure stretching motions along the bond Cl···H and C_{α}···H. Both transition states are separated by 7.32 kcal/mol, being $TS1_{ax}$ the most stable transition state.

If the attack of Cl atoms occurs in β position, two transition states are possible, namely TS2 equatorial ($TS2_{eq}$) and TS2 axial ($TS2_{ax}$). Both TS2 are characterized by an imaginary frequency with values of 748*i* and 923*i* cm^{-1}, respectively, and corresponding with a pure stretching motion Cl···H and C_{β}···H bond. In this case, $TS2_{ax}$ is 0.48 kcal/mol more stable than $TS2_{eq}$.

Finally, when atomic chlorine approaches the hydrogen atoms in γ position, two transition states TS3 can be formed ($TS3_{eq}$ and $TS3_{ax}$). The characteristic frequencies are 790*i* and 833*i* cm^{-1}, respectively. These frequencies correspond to a pure stretching motion like in the previous case (TS1 and TS2). Both transition state are separated by 0.43 kcal/mol, being $TS3_{ax}$ more stable than $TS3_{eq}$.

The most important structural parameters of TS1, TS2, and TS3 are summarized in Fig. 2. Table 2 shows the energy of transition states evaluated at QCISD(T)/6-31G* level of calculation. In all cases, the attack on the H-axial is favoured against the equatorial one. According to the calculated energy barriers, the most favourable reaction pathway is that going through $TS1_{ax}$, with activation energy of 0.55 kcal/mol, which is more than 5 kcal/mol lower than the value obtained for $TS3_{ax}$. The TS2 reaction pathway is the energetically least favoured.

Table 2
Thermodynamics parameters calculated QCISD(T)/6-31G*//MP2/6-31G* for the different possible pathways in kcal/mol at 298.15 K (see text). The abbreviations ax and eq are referred to axial and equatorial transition states, respectively.

	$TS1_{eq}$	$TS1_{ax}$	$TS2_{eq}$	$TS2_{ax}$	$TS3_{eq}$	$TS3_{ax}$
E_a	7.87	0.55	7.97	7.49	6.28	5.85
$E_{a\ classic}$	10.21	2.24	10.24	9.95	8.52	8.16
$\Delta G^{\neq}$	2.19	−4.61	2.49	2.12	0.86	0.65
$\Delta H_{reac.}$	3.87	3.87	7.97	8.46	6.70	6.70
$\Delta G_{reac.}$	−9.97	−9.97	−6.13	−5.95	−7.33	−7.33

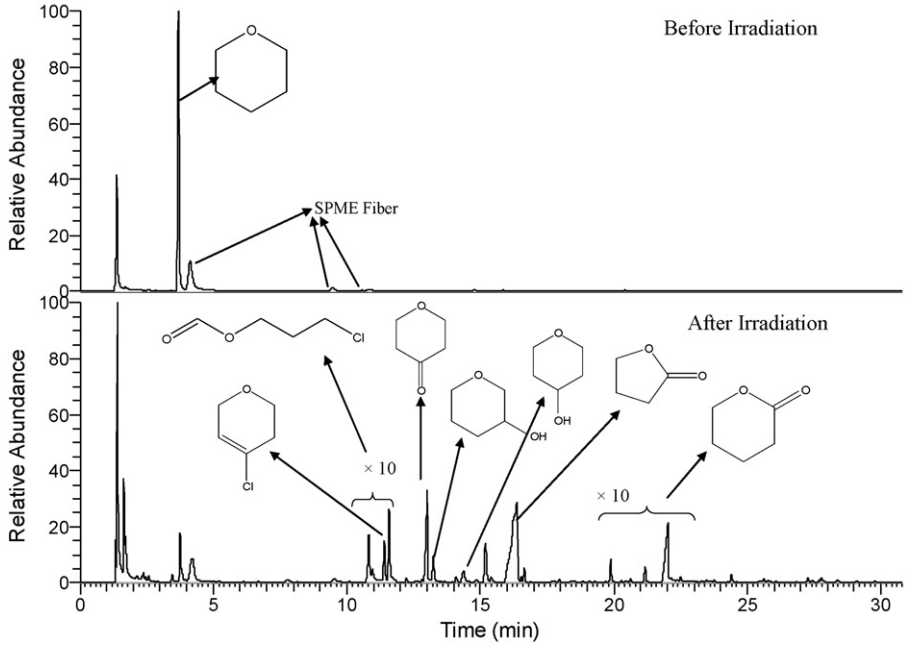

Fig. 3. Gas chromatograms of a sample of $SOCl_2$/THP/air reaction mixture before radiation (upper) and after 83 s of photolysis (lower).

In the light of the energy calculated for the highest occupied molecular orbital (HOMO), α and β, we firstly note that MP2 and QCISD(T) values are in excellent agreement. Comparing the HOMO energies of the α orbital for the different reaction pathways, the values for $TS1_{ax}$ and $TS3_{eq}$ are −0.354 and −0.365 hartree molecule^{-1}, respectively, which are less stable than the average value for the rest of transition states, i.e., -0.375 ± 0.002 hartree molecule^{-1} (where the indicated error is $\pm\sigma$). For the β orbital, the average of the HOMO energy for all transition states is -0.424 ± 0.003 hartree molecule^{-1}. Also, the HOMO energy difference between the α and β orbitals was 0.072 and 0.064 hartree molecule^{-1} for $TS1_{ax}$ and $TS3_{eq}$, respectively, and 0.048 ± 0.002 hartree molecule^{-1} for the rest of transition states. The instability of α orbital shown in this analysis is indicative of the reactivity of the transition state.

In addition, the Mulliken charges were calculated for Cl, H, C, and O atoms in all transition states by MP2 and QCISD(T) methods. Results from both methods are in excellent agreement. For chlorine atoms, the calculated Mulliken charge in $TS1_{ax}$ was −0.255 units, which is more negative than the average value obtained for the rest of transition states (-0.220 ± 0.006 units). In contrast, the Mulliken charge on the hydrogen atom in all transition states was positive (0.058 units for $TS1_{eq}$ and $TS1_{ax}$, and 0.076 ± 0.005 units for the rest of TS). In the case of the carbon atoms involved in the reaction, we have three groups of values. The two first sets of values involve TS1 transition states, i.e., 0.084 and 0.118 units for the axial and equatorial forms, respectively, while the last group of transition states has an average value of -0.240 ± 0.005 units. Finally, in the case of the oxygen atom, we also get two groups of values, one involves the TS1 transition states and yields an average value of -0.588 ± 0.005 units and for the rest of transition states the averaged value calculated was -0.622 ± 0.005 units. This analysis shows that the role of the oxygen atoms of THP in TS1 transition states is expected to be important.

Finally, considering the calculated enthalpies or free energies of reaction, a similar conclusion was found than that with the calculated energy barriers. From the reaction enthalpies point of view (Table 2), the most favourable reaction channels are expected to be those involving TS1 (3.87 kcal mol^{-1}), while processes proceeding via TS3 (6.70 kcal mol^{-1}) and TS2 (8.46 and 7.97 kcal mol^{-1} for the axial and equatorial attacks, respectively) are less favourable. Moreover, in terms of the free energy of reaction, the most favourable reaction channel is that proceeding via TS1 transition states (−9.97 kcal mol^{-1}), being the least favourable reaction pathway that involving $TS2_{ax}$ (−5.95 kcal mol^{-1}).

4.3. Reaction products and mechanism

Mechanistic studies have shown that the OH-initiated oxidation of cyclic ethers under atmospheric conditions leads, in general, to ring opening with the resultant radicals containing the formate functional group [8,10,37,38]. The OH reaction proceeds by H-atom abstraction, followed by reaction with O_2 and NO, to form a cyclic alkoxy radical, which decomposes through C–C cleavage. In the case of Cl-initiated oxidation of ethers, Starkey et al. [39] reported for the reaction of Cl with methylethylether that the main attack occurs in the α position.

An example of the gas chromatogram before and after irradiati on of a THP/Cl precursor/air mixture is shown in Fig. 3. As can be seen in the lower panel of the figure, the relative abundance of THP decreased in the course of the reaction respect to that shown

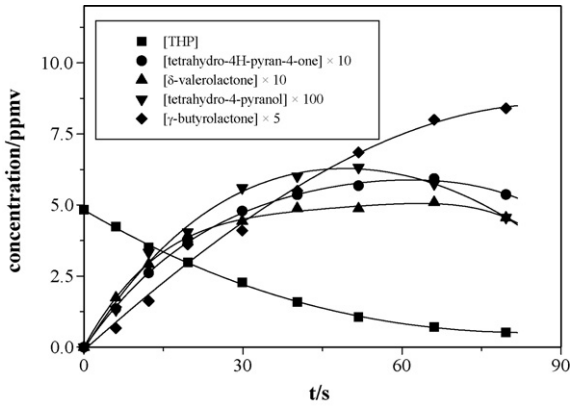

Fig. 4. Plot of the concentration of product and THP versus the time of reaction. Analyses were carried out by SPME/GC–MS.

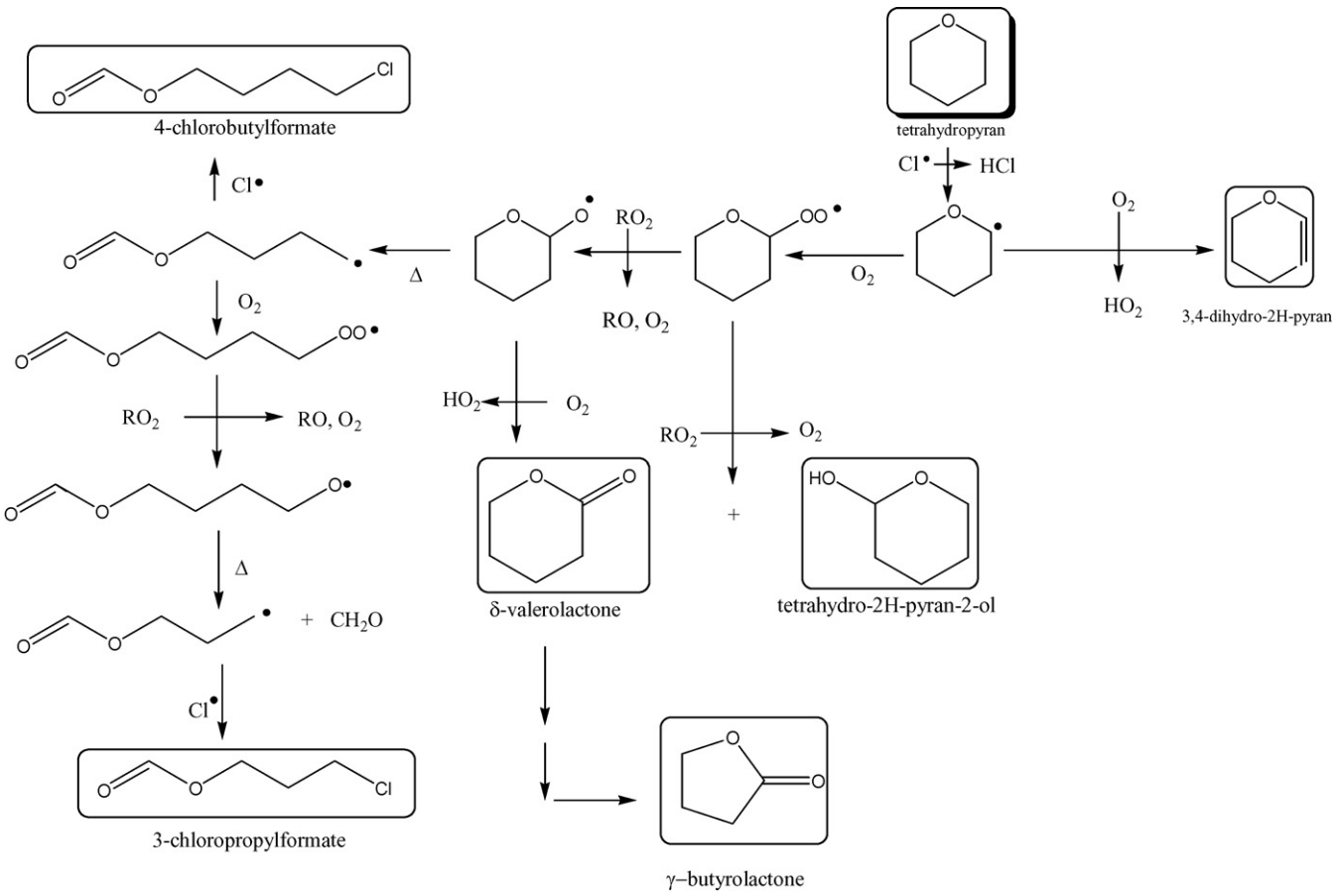

Scheme 1. Proposed mechanism for the attack of Cl atoms to α-H of THP, where detected products are shown in a box.

in the upper panel. Several reaction products were also observed in the chromatogram. The major products detected in the reaction of Cl atoms with THP under atmospheric conditions (298 ± 2 K and 740 ± 5 Torr of air) were tetrahydro-2H-pyran-2-one (δ-valerolactone) and tetrahydro-4H-pyran-4-one. Other minor reaction products identified were tetrahydro-2H-pyran-2ol, dihydrofuran-2(3H)-one (γ-butyrolactone), 3,4-dihydro-2H-pyran, 4-chlorobutylformate, 3-chloropropylformate, tetrahydro-2H-pyran-3-ol, dihydro-2H-pyran-3(4H)-one, tetrahydro-4H-pyran-4-ol, and 4-chloro-3,6-dihydro-2H-pyran.

The temporal evolution of THP and main reaction products (δ-valerolactone, tetrahydro-4H-pyran-4-one, tetrahydro-4-pyranol, and γ-butyrolactone) is shown in Fig. 4. The concentration profiles of δ-valerolactone, tetrahydro-4H-pyran-4-one, and tetrahydro-4-pyranol show that all are primary products. However, the profile of γ-butyrolactone seems to indicate that it is a secondary product.

The reaction of Cl atoms with THP can proceed by H-abstraction from three different positions with respect to the O atom. Scheme 1 shows the proposed mechanism for the attack of Cl in the α position that would justify the observed reaction products (shown included in a box). After H abstraction by Cl atoms, the addition of a molecule of oxygen to the α-tetrahydropyran radical yields the corresponding peroxy radical which can react with itself or with other RO_2 [40,41] to form δ-valerolactone and tetrahydro-2H-pyran-2-ol. The peroxy radical can also form cyloalkoxy radicals that can further react with O_2 to also give the observed δ-valerolactone and HO_2.

The concentration profile of the reactive primary product can be described by the following expression [42]:

$$\frac{[\text{product}]}{[\text{THP}]_0} = \frac{\alpha(1-x)\{(1-x)^{k_{\text{rel}}-1}-1\}}{\{1-k_{\text{rel}}\}} \quad (4)$$

where α is the yield of the product formed in the reaction of Cl atoms with THP in the presence of oxygen, $x = 1 - ([\text{THP}]/[\text{THP}]_0)$ is the fractional consumption of THP, and k_{rel} is the relative rate coefficient of the product + Cl reaction respect to the THP + Cl reaction. The fit of the experimental data for δ-valerolactone to this equation gives $\alpha = 0.229 \pm 0.015$ and $k_{\text{rel}} = 0.461 \pm 0.015$, where quoted error is twice the standard deviation.

The formation of γ-butyrolactone can be explained by the cleavage of the ring of the δ-valerolactone, the loss of a C atom, and the cyclization. δ-Valerolactone presents an acetate type group in its structure and could form the α-radical respect to the oxygen into the ring which could form a peroxy radical and, subsequently, an alkoxy radical in the presence of O_2. This alkoxy radical could open the ring via a C–O bond cleavage. The linear product formed could eliminate CO_2 (reaction (5)) similarly to the mechanism proposed by Christensen et al. [43] in the reaction of methyl acetate with Cl atoms. These authors have found that this reaction proceeded more than 95% via H-abstraction at the $-OCH_3$ site. In our reaction, the remaining radical after the CO_2 elimination could form the corresponding linear alkoxy radical in the presence of O_2:

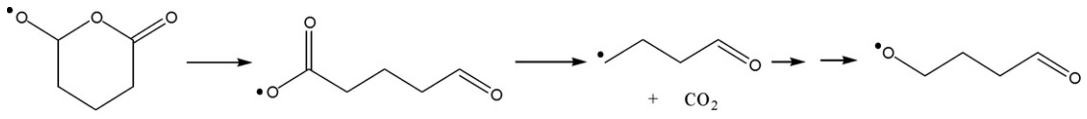

(5)

The linear alkoxy radical formed in the sequence of reaction (5) could form a five membered ring by cyclization, which could finally give the observed γ-butyrolactone:

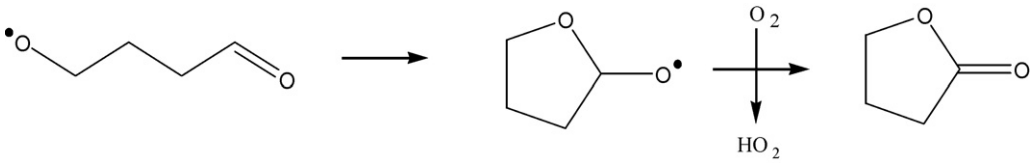

(6)

In order to corroborate this proposed mechanism additional experiments were performed on the reaction of δ-valerolactone with Cl atoms. γ-Butyrolactone was found to be the main reaction product. Additionally, if the experimental data of the concentration of γ-butyrolactone are fitted to the Eq. (4) a negative k_{rel} is obtained, showing that the γ-butyrolactone is not a primary product of reaction (1).

The formation of furan derivatives by cyclization of linear alkoxy radicals has also been proposed by Baker et al. [44] in the reaction of OH radical with a series of 1,4-hydroxyketones.

Other minor products detected from the α-attack of Cl to THP are 3,4-dihydro-2H-pyran, 4-chlorobutylformate, and 3-chloropropylformate. As can be seen in Scheme 1, 3,4-dihydro-2H-pyran can be formed in the reaction of O_2 with the α-cyclic radical produced in the first step of the Cl reaction. Moreover, as mentioned before, formates are characteristic products observed in the reaction of cyclic ethers and OH radical, under atmospheric conditions [8,10,37,38]. These mechanistic studies propose the ring opening as a first step in the formation of the radicals containing the formate functional group. A similar mechanism is proposed in Scheme 1 for the formation of the chloroformate products detected in this work.

Scheme 2 shows the proposed mechanism for the Cl attack to the CH_2 group in β position and the detected products from this attack. Tetrahydro-2H-pyran-3-ol and dihydro-2H-pyran-3(4H)-one were detected as minor products of reaction (1). The pyranol can be formed in the reaction of the β-peroxy radical with RO_2, and the pyranone can also be formed from the β-alkoxy radical as Scheme 2 shows.

Tetrahydro-4H-pyran-4-one, tetrahydro-4H-pyran-4-ol, and 4-chloro-3,6-dihydro-2H-pyran have been identified in this work. Scheme 2 shows the proposed mechanism for the attack of Cl to the γ position of THP which justifies our observations. Tetrahydro-4H-pyran-4-one together with δ-valerolactone are the main products observed in this study of reaction (1). Quantification of tetrahydro-4H-pyran-4-one, using Eq. (4), gives a yield of 0.206 ± 0.007 and $k_{rel} = 0.317 \pm 0.035$. This product could be formed in the reaction of

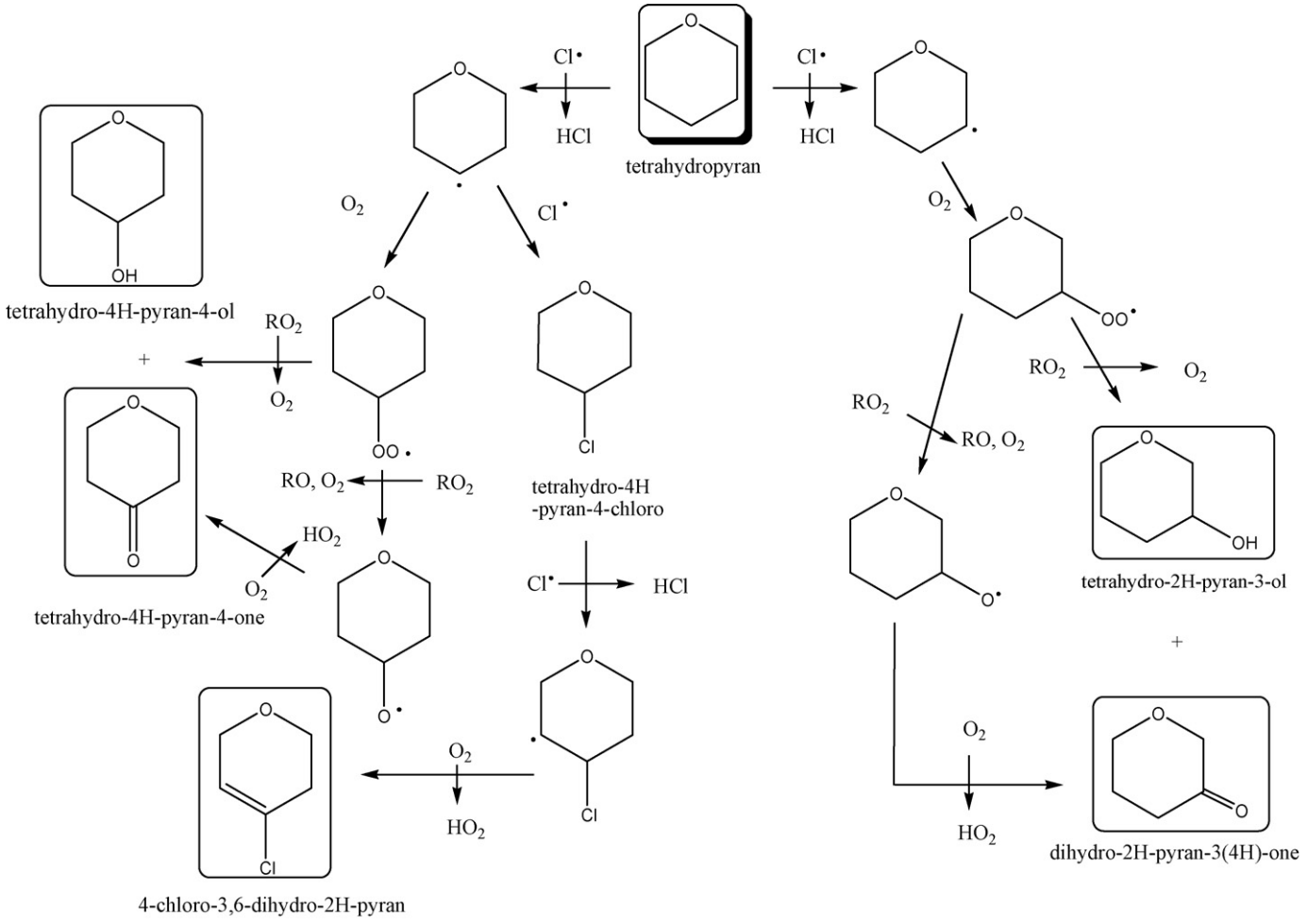

Scheme 2. Proposed mechanism for the attack of Cl atoms to β-H and γ-H of THP, where detected products are shown in a box.

the γ-alkoxy cyclic radical with O_2 or by reaction of the peroxy-cycled radical with RO_2 giving a mixture of the pyranone and the pyranol. The calculated yield from the fit of the temporal profile of tetrahydro-4H-pyran-4-ol to Eq. (4) is 0.028 ± 0.002 and $k_{rel} = 0.510 \pm 0.067$. These results show that the main production pathway of the pyranone is from the alkoxy cyclic radical. 4-Chloro-3,6-dihydro-2H-pyran is also a minor product detected that could be formed in the reaction of the γ radical with Cl atoms (Scheme 2).

Scheme 2 does not show ring opening routes because products that require this route of reaction have not been detected. As previously explained this ring opening is only produced in the radicals with the acetate group.

In general, the yields of the carbonyls are significantly higher than those for the corresponding alcohols because the carbonyls can also be produced from the reaction of the cyclic oxy radical with molecular oxygen, as can be see in the Schemes. Total molar product yields that were found in the investigation presented here was 46.3%.

According to the reaction products observed in this study, all reaction pathways proceed by H-abstraction and hydrogen chloride was detected by FTIR experiments as a final product of reaction (1). The experimental product studies performed confirm that there is a competition between α and γ attacks. The α attack is the most favoured channel in concordance with the *ab initio* calculations presented in the previous subsection. However, the experimental product study also indicates that the γ and β attacks cannot be considered negligible.

5. Atmospheric implications

Volatile organic compounds, in general, are chemically removed from the troposphere mainly by their reaction with OH, NO_3, O_3, and halogen atoms. The tropospheric lifetime of THP due to its reaction with Cl atoms (defined as $\tau = 1/k_1[Cl]$) can be estimated by using a concentration of 10^5 atoms cm^{-3} (peak value observed under specific circumstances in marine regions) [16]. Under these local conditions, THP is expected to be removed by Cl atoms in 12.6 h. However, on a global scale, Rudolph et al. [45] estimated upper limits of the average tropospheric Cl atom concentration of less than 10^3 atoms cm^{-3} for the Northern hemisphere and nearly 2×10^3 atoms cm^{-3} for the Southern hemisphere. These concentrations yield lifetimes between 52.3 and 26.2 days for the atmospheric disappearance of THP by the reaction with Cl atoms.

To our knowledge, there are no bibliographic references for the reaction of THP with NO_3 radicals and O_3. In contrast, two studies of the rate coefficients for the reaction of THP with OH radicals have been reported at 298 ± 2 K [9,10]. Assuming the average value of these rate coefficients (1.23×10^{-11} cm^3 $molecule^{-1}$ s^{-1}) and using an OH concentration (24-h averaged) of 10^6 radicals cm^{-3} [46], the calculated tropospheric lifetime for THP due to the reaction with OH radicals is 23.3 h.

In the light of these results, we can conclude that the reaction with chlorine atoms can provide an effective tropospheric loss pathway for THP under specific circumstances. This reaction is expected to play a significant role in the tropospheric chemistry of the marine boundary layer, in coastal urban areas, and in some contaminated urban areas (where levels of chlorine may be originated from industrial emissions) where the Cl concentration peaks at dawn, much earlier than OH does.

Acknowledgements

The authors would like to thank Dr. Alberto Notario and Prof. Manuel Fernández for the valuable suggestions made. They also thank the Spanish Ministerio de Educación y Ciencia (Projects CGL2004-03355/CLI and CGL2007-61835) and the Junta de Comunidades de Castilla-La Mancha (Projects PAI-05-062 and PCI08-0123-0381) for the financial support of this research work. A.A. Ceacero-Vega wishes to thank the first institution for the grant provided.

References

[1] J.J. Orlando, The atmospheric oxidation of diethyl ether: chemistry of the C_2H_5–O–CH(O•)CH_3 radical between 218 and 335 K, Phys. Chem. Chem. Phys. 9 (2007) 4189–4199.
[2] K. Enomoto, Y. Maekawa, Y. Katsumura, T. Miyazaki, M. Yoshida, H. Hamana, T. Narita, Radiation-induced radical polyaddition of bis(alpha-trifluoromethyl-beta,beta-difluorovinyl) terephthalate with excess of various ethers, Macromolecules 38 (2005) 9584–9593.
[3] D.W. Harney, T.A. Macrides, Synthesis of an isomeric mixture (24RS,25RS) of sodium scymnol sulfate, Steroids 73 (2008) 424–429.
[4] M.A. Hiebel, B. Pelotier, P. Goekjian, O. Piva, 2,6-Disubstituted tetrahydropyrans by tandem cross-metathesis/Iodocyclisation, Eur. J. Org. Chem. (2008) 713–720.
[5] A.R. Katritzky, A.A.A. Abdel-Fattah, K.R. Idzik, B. El-Gendy, J. Soloducho, Benzotriazole-mediated alkoxyalkylation and acyloxyalkylation, Tetrahedron 63 (2007) 6477–6484.
[6] K. Washida, T. Koyama, K. Yamada, M. Kita, D. Uemura, Karatungiols A and B, two novel antimicrobial polyol compounds, from the symbiotic marine dinoflagellate Amphidinium sp., Tetrahedron Lett. 47 (2006) 2521–2525.
[7] T. Kubota, Y. Sakuma, K. Shimbo, M. Tsuda, M. Nakano, Y. Uozumi, J. Kobayashi, A. Amphezonol, A novel polyhydroxyl metabolite from marine dinoflagellate Amphidinium sp., Tetrahedron Lett. 47 (2006) 4369–4371.
[8] A. Mellouki, G. Le Bras, H. Sidebottom, Kinetics and mechanisms of the oxidation of oxygenated organic compounds in the gas phase, Chem. Rev. 103 (2003) 5077–5096.
[9] P. Dagaut, R.Z. Liu, T.J. Wallington, M.J. Kurylo, Flash-photolysis resonance fluorescence investigation of the gas-phase reactions of hydroxyl radicals with cyclic ethers, J. Phys. Chem. 94 (1990) 1881–1883.
[10] J. Moriarty, H. Sidebottom, J. Wenger, A. Mellouki, G. Le Bras, Kinetic studies on the reactions of hydroxyl radicals with cyclic ethers and aliphatic diethers, J. Phys. Chem. A 107 (2003) 1499–1505.
[11] B.T. Jobson, H. Niki, Y. Yokouchi, J. Bottenheim, F. Hopper, R. Leaitch, Measurements of C-2–C-6 hydrocarbons during the polar sunrise 1992 experiment—evidence for Cl atom and Br atom chemistry, J. Geophys. Res. 99 (1994) 25355–25368.
[12] H.B. Singh, A.N. Thakur, Y.E. Chen, M. Kanakidou, Tetrachloroethylene as an indicator of low Cl atom concentrations in the troposphere, Geophys. Res. Lett. 23 (1996) 1529–1532.
[13] A.D. Keil, P.B. Shepson, Chlorine and bromine atom ratios in the springtime Arctic troposphere as determined from measurements of halogenated volatile organic compounds, J. Geophys. Res. 111 (2006).
[14] A.E. Cavender, T.A. Biesenthal, J.W. Bottenheim, P.B. Shepson, Volatile organic compound ratios as probes of halogen atom chemistry in the Arctic, Atmos. Chem. Phys. 8 (2008) 1737–1750.
[15] B.J. Finlayson-Pitts, J.N. Pitts, Chemistry of the Upper and Lower Atmosphere, Academic Press, San Diego, 1999.
[16] C.W. Spicer, E.G. Chapman, B.J. Finlayson-Pitts, R.A. Plastridge, J.M. Hubbe, J.D. Fast, C.M. Berkowitz, Unexpectedly high concentrations of molecular chlorine in coastal air, Nature 394 (1998) 353–356.
[17] A.A.P. Pszenny, W.C. Keene, D.J. Jacob, S. Fan, J.R. Maben, M.P. Zetwo, M. Springeryoung, J.N. Galloway, Evidence of inorganic chlorine gases other than hydrogen-chloride in marine surface air, Geophys. Res. Lett. 20 (1993) 699–702.
[18] G.A. Impey, P.B. Shepson, D.R. Hastie, L.A. Barrie, K.G. Anlauf, Measurements of photolyzable chlorine and bromine during the Polar sunrise experiment 1995, J. Geophys. Res. Atmos. 102 (1997) 16005–16010.
[19] E. Galan, I. Gonzalez, B. Fabbri, Estimation of fluorine and chlorine emissions from Spanish structural ceramic industries. The case study of the Bailen area, Southern Spain, Atmos. Environ. 36 (2002) 5289–5298.
[20] B. Ballesteros, A. Garzon, E. Jimenez, A. Notario, J. Albaladejo, Relative and absolute kinetic studies of 2-butanol and related alcohols with tropospheric Cl atoms, Phys. Chem. Chem. Phys. 9 (2007) 1210–1218.
[21] IUPAC, Subcommittee on gas kinetic data evaluation, Evaluated kinetic data, http://www.iupac-kinetic.ch.cam.ac.uk/, 2009.
[22] M.L. Ragains, B.J. Finlayson-Pitts, Kinetics and mechanism of the reaction of Cl atoms with 2-methyl-1,3-butadiene (isoprene) at 298 K, J. Phys. Chem. A 101 (1997) 1509–1517.
[23] J.J. Orlando, G.S. Tyndall, E.C. Apel, D.D. Riemer, S.E. Paulson, Rate coefficients and mechanisms of the reaction of Cl-atoms with a series of unsaturated hydrocarbons under atmospheric conditions, Int. J. Chem. Kinet. 35 (2003) 334–353.
[24] C.L. Arthur, J. Pawliszyn, Solid-phase microextraction with thermal-desorption using fused-silica optical fibers, Anal. Chem. 62 (1990) 2145–2148.
[25] M.D. Alpendurada, Solid-phase microextraction: a promising technique for sample preparation in environmental analysis, J. Chromatogr. A 889 (2000) 3–14.
[26] K. Treves, Y. Rudich, The atmospheric fate of C-3–C-6 hydroxyalkyl nitrates, J. Phys. Chem. A 107 (2003) 7809–7817.

[27] G.E. Orzechowska, S.E. Paulson, Photochemical sources of organic acids. 1. Reaction of ozone with isoprene, propene, and 2-butenes under dry and humid conditions using SPME, J. Phys. Chem. A 109 (2005) 5358–5365.
[28] F. Reisen, S.M. Aschmann, R. Atkinson, J. Arey, 1,4-Hydroxycarbonyl products of the OH radical initiated reactions of C-5–C-8 n-alkanes in the presence of NO, Environ. Sci. Technol. 39 (2005) 4447–4453.
[29] J. Baker, J. Arey, R. Atkinson, Rate constants for the gas-phase reactions of OH radicals with a series of hydroxyaldehydes at 296 ± 2 K, J. Phys. Chem. A 108 (2004) 7032–7037.
[30] F. Villanueva, I. Barnes, E. Monedero, S. Salgado, M.V. Gomez, P. Martin, Primary product distribution from the Cl-atom initiated atmospheric degradation of furan: environmental implications, Atmos. Environ. 41 (2007) 8796–8810.
[31] G.W.T.M.J. Frisch, H.B. Schlegel, G.E. Scuseria, M.A. Robb, J.R. Cheeseman, J.A. Montgomery Jr., T. Vreven, K.N. Kudin, J.C. Burant, J.M. Millam, S.S. Iyengar, J. Tomasi, V. Barone, B. Mennucci, M. Cossi, G. Scalmani, N. Rega, G.A. Petersson, H. Nakatsuji, M. Hada, M. Ehara, K. Toyota, R. Fukuda, J. Hasegawa, M. Ishida, T. Nakajima, Y. Honda, O. Kitao, H. Nakai, M. Klene, X. Li, J.E. Knox, H.P. Hratchian, J.B. Cross, V. Bakken, C. Adamo, J. Jaramillo, R. Gomperts, R.E. Stratmann, O. Yazyev, A.J. Austin, R. Cammi, C. Pomelli, J.W. Ochterski, P.Y. Ayala, K. Morokuma, G.A. Voth, P. Salvador, J.J. Dannenberg, V.G. Zakrzewski, S. Dapprich, A.D. Daniels, M.C. Strain, O. Farkas, D.K. Malick, A.D. Rabuck, K. Raghavachari, J.B. Foresman, J.V. Ortiz, Q. Cui, A.G. Baboul, S. Clifford, J. Cioslowski, B.B. Stefanov, G. Liu, A. Liashenko, P. Piskorz, I. Komaromi, R.L. Martin, D.J. Fox, T. Keith, M.A. Al-Laham, C.Y. Peng, A. Nanayakkara, M. Challacombe, P.M.W. Gill, B. Johnson, W. Chen, M.W. Wong, C. Gonzalez, J.A. Pople, Gaussian 03, Revision C.02, Gaussian, Inc., Wallingford, CT, 2004.
[32] Y.Y. Chuang, E.L. Coitino, D.G. Truhlar, How should we calculate transition state geometries for radical reactions? The effect of spin contamination on the prediction of geometries for open-shell saddle points, J. Phys. Chem. A 104 (2000) 446–450.
[33] A. Garzon, C.A. Cuevas, A.A. Ceacero, A. Notario, J. Albaladejo, M. Fernandez-Gomez, Atmospheric reactions Cl + CH_3-(CH_2)(n)-OH (n = 0–4): a kinetic and theoretical study, J. Chem. Phys. 125 (2006) 104305.
[34] A. Garzon, A. Notario, J. Albaladejo, T. Pena-Ruiz, M. Fernandez-Gomez, An experimental and theoretical study of the reaction of ethanethiol with Cl atoms, Chem. Phys. Lett. 438 (2007) 184–189.
[35] M.L. Coote, Reliable theoretical procedures for the calculation of electronic-structure information in hydrogen abstraction reactions, J. Phys. Chem. A 108 (2004) 3865–3872.
[36] M.A. Lill, M.C. Hutter, V. Helms, Accounting for environmental effects in ab initio calculations of proton transfer barriers, J. Phys. Chem. A 104 (2000) 8283–8289.
[37] C.G. Sauer, I. Barnes, K.H. Becker, H. Geiger, T.J. Wallington, L.K. Christensen, J. Platz, O.J. Nielsen, Atmospheric chemistry of 1,3-dioxolane: kinetic, mechanistic, and modeling study of OH radical initiated oxidation, J. Phys. Chem. A 103 (1999) 5959–5966.
[38] J. Platz, J. Sehested, O.J. Nielsen, T.J. Wallington, Atmospheric chemistry of trimethoxymethane, $(CH_3O)_3CH$: laboratory studies, J. Phys. Chem. A 103 (1999) 2632–2640.
[39] D.P. Starkey, K.A. Holbrook, G.A. Oldershaw, R.W. Walker, Kinetics of the reactions of hydroxyl radicals (OH) and of chlorine atoms (Cl) with methylethylether over the temperature range 274-345 K, Int. J. Chem. Kinet. 29 (1997) 231–236.
[40] R. Atkinson, Rate constants for the atmospheric reactions of alkoxy radicals: an updated estimation method, Atmos. Environ. 41 (2007) 8468–8485.
[41] R. Atkinson, J. Arey, S.M. Aschmann, Atmospheric chemistry of alkanes: review and recent developments, Atmos. Environ. 42 (2008) 5859–5871.
[42] R.J. Meagher, M.E. McIntosh, M.D. Hurley, T.J. Wallington, A kinetic study of the reaction of chlorine and fluorine atoms with HC(O)F at 295 ± 2 K, Int. J. Chem. Kinet. 29 (1997) 619–625.
[43] L.K. Christensen, J.C. Ball, T.J. Wallington, Atmospheric oxidation mechanism of methyl acetate, J. Phys. Chem. A 104 (2000) 345–351.
[44] J. Baker, J. Arey, R. Atkinson, Rate constants for the reactions of OH radicals with a series of 1,4-hydroxyketones, J. Photochem. Photobiol. A: Chem. 176 (2005) 143–148.
[45] J. Rudolph, R. Koppmann, C. PlassDulmer, The budgets of ethane and tetrachloroethene: is there evidence for an impact of reactions with chlorine atoms in the troposphere? Atmos. Environ. 30 (1996) 1887–1894.
[46] H.P. Dorn, U. Brandenburger, T. Brauers, M. Hausmann, D.H. Ehhalt, In-situ detection of tropospheric OH radicals by folded long-path laser absorption. Results from the POPCORN field campaign in August 1994, Geophys. Res. Lett. 23 (1996) 2537–2540.